The Role of β-Arg-182, an Essential Catalytic Site Residue in *Escherichia coli* F_1-ATPase

Sashi Nadanaciva, Joachim Weber, and Alan E. Senior*

Department of Biochemistry and Biophysics, Box 712, University of Rochester Medical Center, Rochester, New York 14642

Received March 22, 1999

ABSTRACT: β-Arg-182 in *Escherichia coli* F_1-ATPase (β-Arg-189 in bovine mitochondrial F_1) is a residue which lies close to catalytic site bound nucleotide (Abrahams et al. (1994) *Nature 370*, 621−628). Here we investigated the role of this residue by characterizing two mutants, βR182Q and βR182K. Oxidative phosphorylation and steady-state ATPase activity of purified F_1 were severely impaired by both mutations. Catalytic site nucleotide-binding parameters were measured using the fluorescence quench of β-Trp-331 that occurred upon nucleotide binding to purified F_1 from βR182Q/βY331W and βR182K/βY331W double mutants. It was found that (a) β-Arg-182 interacts with the γ-phosphate of MgATP, particularly at catalytic sites 1 and 2, (b) β-Arg-182 has no functional interaction with the β-phosphate of MgADP or with the magnesium of the magnesium−nucleotide complex in the catalytic sites, and (c) β-Arg-182 is directly involved in the stabilization of the catalytic transition state. In these features the role of β-Arg-182 resembles that of another positively charged residue in the catalytic site, the conserved lysine of the Walker A motif, β-Lys-155. A further role of β-Arg-182 is suggested, namely involvement in conformational change at the catalytic site β−α subunit interface that is required for multisite catalysis.

The bulk of ATP, the energy currency of cells, is synthesized by ATP synthase (also called F_1F_o-ATPase) found in bacteria, chloroplasts, and mitochondria (*1*, *2*). This enzyme synthesizes ATP from ADP and P_i using a proton motive force and can function in the reverse direction in bacteria, hydrolyzing ATP to generate a proton gradient for nutrient uptake and locomotion. A structurally complicated protein, ATP synthase consists of a peripheral portion, F_1, which has three catalytic sites, and a hydrophobic membrane-spanning portion, F_o, which acts as a proton conducting pathway.

The intricate catalytic mechanism of ATP synthase has been made more amenable for study by the use of a simpler experimental system, solubilized F_1, which exhibits ATPase activity in the absence of F_o. F_1 contains 5 types of subunits in the stoichiometry $\alpha_3\beta_3\gamma\delta\epsilon$. The catalytic sites lie at the three β−α interfaces with most of the amino acid residues which ligand to nucleotide being contributed by the β subunits (*3*). These sites differ from each other in their conformation at any given moment during catalysis (*2*), and this asymmetry is induced by the γ subunit rotating within the $\alpha_3\beta_3$ hexagon (*4*, *5*) and by the residues which ligand to magnesium in the Mg−nucleotide in the catalytic sites (*6*). The three catalytic sites act sequentially, carrying out catalysis with strong positive cooperativity (*2*, *7*, *8*). At substoichiometric concentrations, substrate MgATP binds very tightly to just one catalytic site, and under these single-turnover or "unisite" conditions the equilibrium constant for the hydrolysis reaction is close to unity and product release is very slow (*8*). At cellular concentrations of MgATP, all three catalytic sites are filled and catalysis is accelerated 10^5-fold to achieve physiological rates (*2*). Catalysis fails to occur in the absence of Mg, and uncomplexed (free) nucleotide binds to all three catalytic sites with equal, relatively low affinity (*6*).

Recent X-ray structures of F_1 from bovine mitochondria (*3*), rat liver mitochondria (*9*), and the $\alpha_3\beta_3$ complex from the thermophilic bacterium PS3 (*10*) have advanced our understanding of the structure of the catalytic sites. By using these X-ray structures as a foundation and by genetically engineering tryptophan residues into the catalytic sites to act as intrinsic fluorescent probes sensitive to nucleotide binding (*11*−*13*), our laboratory has investigated essential catalytic site residues in *Escherichia coli* F_1. Several residues have been found that coordinate magnesium (*14*), several directly provide binding energy for nucleotide substrate (*15*), and some stabilize the transition state (*16*).

One of the residues seen in the environment of catalytic site-bound nucleotide in F_1 is β-Arg-182.[1] As revealed in the MgAMPPNP-containing catalytic site of bovine mitochondrial F_1 (*3*), a nitrogen of the guanidinium group of β-Arg-182 (β-Arg-189 in bovine F_1) lies 3.3 Å from the nearest oxygen of the γ-phosphate of MgAMPPNP (Figure 1). An essential role of this Arg in catalysis was indicated by the work of Park et al. (*17*) who showed that the replacement with either glutamine or alanine caused the loss of both ATPase and ATP synthase activity. In the present paper, we analyzed the role of β-Arg-182 in detail by characterizing two double mutants, βR182Q/βY331W and βR182K/βY331W. The Tyr residue at β-331 makes van der Waals contact with the adenine ring in the catalytic site (*15*), and replacement of Tyr by Trp results in active enzyme with k_{cat}/K_m similar to wild-type. The inserted Trp has a strong fluorescent signal that is quenched completely upon binding of nucleotide at the catalytic site (*11*). This enabled us to measure binding parameters for MgATP, MgADP, free (uncomplexed) ATP, and ADP at the catalytic sites of

[1] *E. coli* residue numbering is used throughout.

10.1021/bi990663x CCC: $18.00
Published on Web 05/26/1999

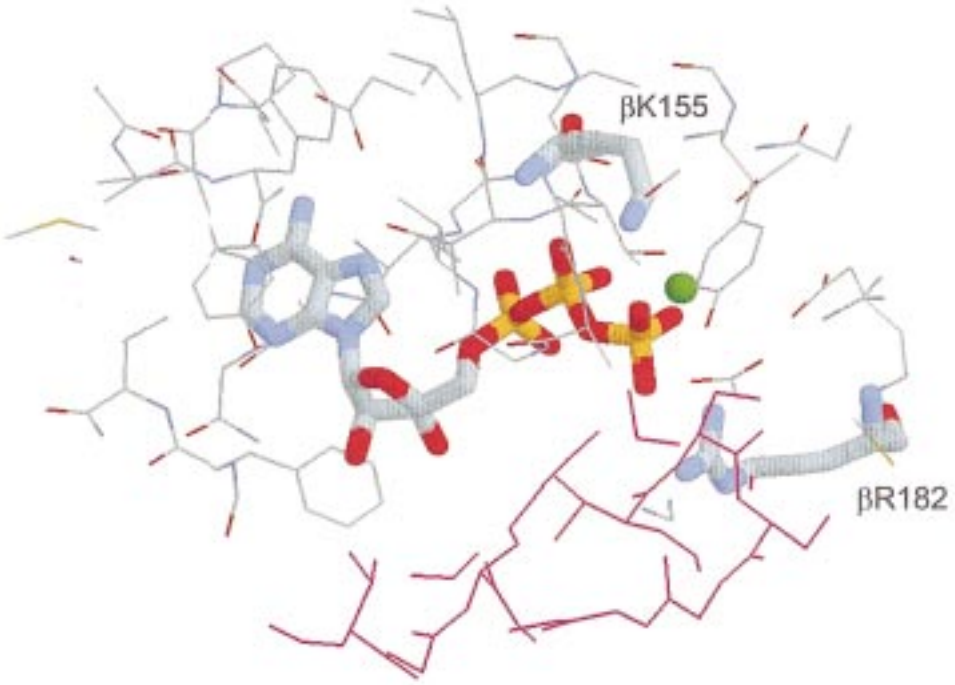

FIGURE 1: The X-ray crystal structure of the catalytic site of F_1-ATPase. β-subunit residues are gray, and α-subunit residues are pink. Positively charged residues β-Arg-182 and β-Lys-155 as well as MgATP (Mg^{2+} is depicted in green) are displayed. This is the "βTP site" of ref *3*; the actual nucleotide in the crystals was MgAMPPNP. (Rasmol software was kindly provided by Roger Sayle, Glaxo Research and Development, Greenford, UK).

purified F_1 from βR182Q/βY331W and βR182K/βY331W mutants. In addition, we tested the ability of F_1 from these mutants to form the catalytic transition state by measuring binding of the transition-state analogue, MgADP−fluoroaluminate.

EXPERIMENTAL PROCEDURES

Construction of Mutant E. coli Strains βR182Q/βY331W and βR182K/βY331W. Site-directed mutagenesis was carried out according to the method of Vandeyar et al. (*18*). Template DNA for generating βR182Q/βY331W and βR182K/βY331W mutations was M13mp18 containing a 2.5 kb *Hin*DIII-*Kpn*I fragment from plasmid pSWM4 (*11*). This fragment contains the βY331W. The mutagenic oligonucleotide for βR182Q was GC GTA GGT GAA **CAG** AC*G* CGT GAG GGT where bold letters are changes made for the mutation Arg → Gln (**CGT → CAG**) and *G* indicates a silent mutation which introduces an *Mlu*I site, used to identify mutant. DNA sequencing confirmed the presence of βR182Q and βY331W mutations and ruled out the presence of any undesired mutation. A 1 kb *Nhe*I-*Fse*I fragment containing βR182Q and βY331W was moved from replicative form phage to plasmid pSWM4 to generate a new plasmid pSN2 (βR182Q/βY331W). pSN2 was introduced into JP17, a strain which contains a deletion in the chromosomal β-subunit gene (*19*), to generate strain SN2.

The mutagenic oligonucleotide for βR182K was GC GTA GGT GAA **AAA** AC*G* CGT GAG GGT, where bold letters are changes made for the mutation Arg → Lys (**CGT → AAA**) and *G* indicates a silent mutation which introduces an *Mlu*I site. Construction of the βR182K/βY331W mutant plasmid, pSN1, was analogous to pSN2 above. However, the yield of F_1 isolated from strain pSN1/JP17 was very low (0.004 mg/g wet wt cells). Recently it was shown that high yields of purified mutant F_1 are obtained using plasmid pBWU13.4 derivatives expressed in strain DK8 (*20*). Therefore a 3.3 kb *Xho*I-*Eag*I fragment in pBWU13.4 was replaced by the corresponding fragment from pSN1 to generate plasmid pSN5 (βR182K/βY331W). pSN5 was introduced into DK8 to generate strain SN5. This strain produced a high yield of mutant F_1 (0.2 mg/g wet wt cells).

Characterization of Mutant E. coli Strains. Growth yields of βR182Q/βY331W and βR182K/βY331W mutant strains in limiting (3 mM) glucose liquid medium and growth tests on solid succinate medium were done as described (*21*).

Enzyme Purification and Characterization. βR182Q/βY331W F_1 from strain SN2, βR182K/βY331W F_1 from strain SN5, βY331W F_1 from strain SWM4 (*11*), and wild-type F_1 from strain SWM1 (*22*) were purified as described in ref *23*. Nucleotide-depleted F_1 (depleted of noncatalytic- and catalytic-site-bound nucleotide) was prepared as described in ref *24*. Enzyme purity and subunit composition were determined by SDS gel electrophoresis (*25*). Protein concentrations were determined by the method of Bradford (*26*). ATPase activity measurements were carried out in 50 mM Tris/SO_4, 10 mM ATP, and 4 mM $MgCl_2$, pH 8.5, at 30 °C, and phosphate release was measured by the method of van Veldhoven and Mannaerts (*27*).

Fluorescence Measurements. An Aminco-Bowman 2 or SPEX-Fluorolog 2 spectrofluorometer was used to measure tryptophan fluorescence. The excitation and emission wavelengths were 295 and 360 nm, respectively. Prior to each nucleotide titration, 100 μL aliquots of F_1 were preequilibrated in 50 mM Tris/SO_4, pH 8, by passage through two 1 mL Sephadex G50 centrifuge columns, thus depleting the catalytic sites of bound nucleotide (*6*). The final concentration of F_1 in the cuvette was 50−100 nM. All fluorescence measurements were done at 23 °C. For MgATP

Table 1: Characterization of *E. coli* Strains and Purified F_1 Containing βR182Q/βY331W and βR182K/βY331W Mutations

mutation	growth yield in limiting glucose (%)	ATPase activity of purified F_1 (units/mg)
wild-type (pDP34N/JP17)	100	28
Unc$^-$ (pUC118/JP17)	54	
βR182Q/βY331W[a]	54	0.003
wild-type (pBWU13.4/DK8)	100	not done
Unc$^-$ (pUC118/DK8)	40	
βR182K/βY331W[a]	45	0.14

[a] The βR182Q/βY331W mutation was expressed in strain JP17, and the βR182K/βY331W mutation was expressed in strain DK8. See Experimental Procedures.

or MgADP titrations, the buffer (50 mM Tris/SO_4, pH 8) contained 2.5 mM $MgSO_4$ with NaATP or NaADP added as indicated. For ATP or ADP titrations, the buffer (50 mM Tris/SO_4, pH 8) contained 0.5 mM EDTA, with NaATP or NaADP added as indicated. For MgADP titrations in the presence of fluoroaluminate, the buffer (50 mM Tris/SO_4, pH 8) contained 2.5 mM $MgSO_4$, 0.5 mM $AlCl_3$, and 5 mM NaF, and NaADP was added at increasing concentrations. Enzyme was preincubated 60 min at room temperature before fluorescence signals were measured to allow full inhibition by fluoroaluminate to be obtained (*16*). Background signals due to buffer were subtracted. Inner filter effects and volume effects were corrected by carrying out parallel titrations with wild-type F_1. Nucleotide-binding parameters were determined from computer-generated fits to the measured data (*15*, *23*).

RESULTS

General. Earlier work (*17*) on βR182Q and βR182A mutants had suggested an essential function for residue β-Arg-182. To gain more detailed information we made the mutants βR182Q/βY331W and βR182K/βY331W. First it was necessary to check the functional properties of these double mutants.

Functional Effects of βR182Q/βY331W and βR182K/βY331W Mutations. Growth yields of mutant strains were tested in liquid medium containing limiting glucose. Table 1 shows that the strain containing βR182Q/βY331W had a growth yield the same as that of the Unc$^-$ control (pUC118/JP17), indicating that the βR182Q mutation abolished ATP synthase activity in vivo. It has been established previously that the βY331W mutation by itself has little effect on growth yield (*11*). The strain containing βR182K/βY331W had a growth yield which exceeded that of the Unc$^-$ control by 5% (Table 1), indicating that ATP synthesis occurs at a very low rate when Arg is replaced by Lys at β-182. Neither mutant strain grew on succinate plates, confirming that the βR182Q and βR182K mutations severely reduced oxidative phosphorylation. Purified F_1 from both mutants had a molecular size similar to that of wild-type F_1, as deduced from the Sephacryl S300 elution profile during the last step of the purification procedure. SDS−polyacrylamide gel electrophoresis of purified F_1 from both of these mutants showed a subunit composition identical to that of wild-type. Table 1 reports specific ATPase activities of purified F_1 from both mutants. βR182Q/βY331W F_1 had very low specific activity equal to 0.01% of wild-type, while βR182K/βY331W F_1 had a specific activity which was 0.5% of wild-type (βY331W F_1 itself has a specific activity which is 50% of that of wild-type F_1; ref *11*).

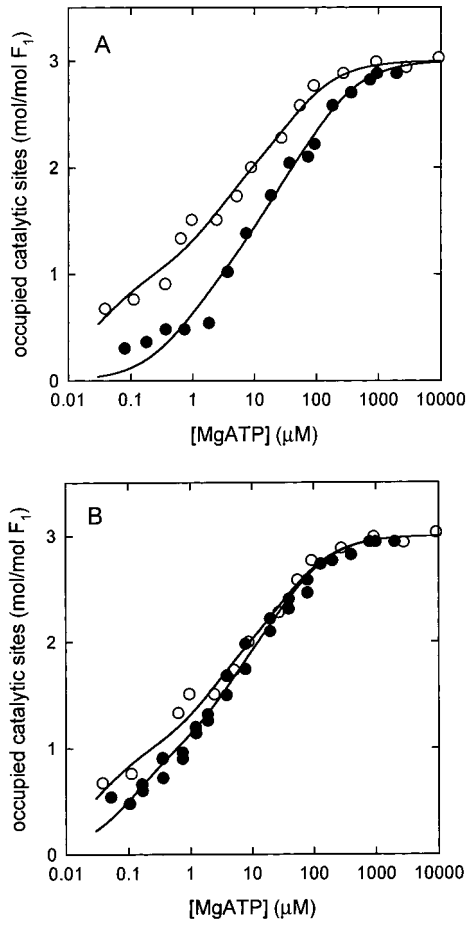

FIGURE 2: MgATP binding to catalytic sites of βR182Q/βY331W and βR182K/βY331W F_1: (A) ●, R182Q/βY331W F_1; ○, βY331W F_1; and (B) ●, βR182K/βY331W F_1; ○, βY331W F_1. The lines are computer-generated fits assuming a model with three different binding sites. Calculated K_d values are given in Table 2. See Experimental Procedures for further details.

Tryptophan Fluorescence Properties of βR182Q/βY331W and βR182K/βY331W F1. The tryptophan fluorescence spectra of purified F_1 from βR182Q/βY331W and βR182K/βY331W were similar to that of βY331W (shown in ref *11*). Saturating amounts of nucleotide quenched the β-Trp-331 fluorescence signals completely, showing that all three catalytic sites became occupied in both mutants and enabling catalytic site nucleotide-binding parameters to be measured.

MgATP Binding to βR182Q/βY331W and βR182K/βY331W F1. The titration curve for MgATP binding to βR182Q/βY331W F_1 (filled circles) and the corresponding curve for βY331W F_1 (open circles) are shown in Figure 2A. The lines are computer-generated fits assuming a model with three different binding sites. Calculated dissociation constants (K_d) are given in Table 2. It is evident from Figure 2A that, while cooperative binding of MgATP was retained, the βR182Q mutation decreased MgATP-binding affinity considerably. The effect was greatest at the highest-affinity site (site 1), where binding affinity for MgATP was reduced by about 30-fold, but changes were also seen at site 2 (K_{d2} increased 6-fold) and at site 3 (K_{d3} increased 3-fold).

Figure 2B shows MgATP binding to βR182K/βY331W F_1. Here, too, a model assuming three different binding sites

Table 2: Catalytic Site Nucleotide Binding Parameters of βR182Q/βY331W, βR182K/βY331W, and βY331W F_1[a]

	βR182Q/βY331W	βR182K/βY331W	βY331W
MgATP			
K_{d1}	0.8	0.14	0.028[b]
K_{d2}	12.8	3.6	2.1
K_{d3}	116	41	39
ATP			
K_{d1},K_{d2},K_{d3}	665	87	71[c]
MgADP			
K_{d1}	0.08	0.05	0.08[d]
K_{d2},K_{d3}	9.3	9.7	14
ADP			
K_{d1},K_{d2},K_{d3}	45	26	28[d]

[a] K_d values are given in micromolar. [b] From ref *14*. [c] From ref *11*. [d] From ref *16*.

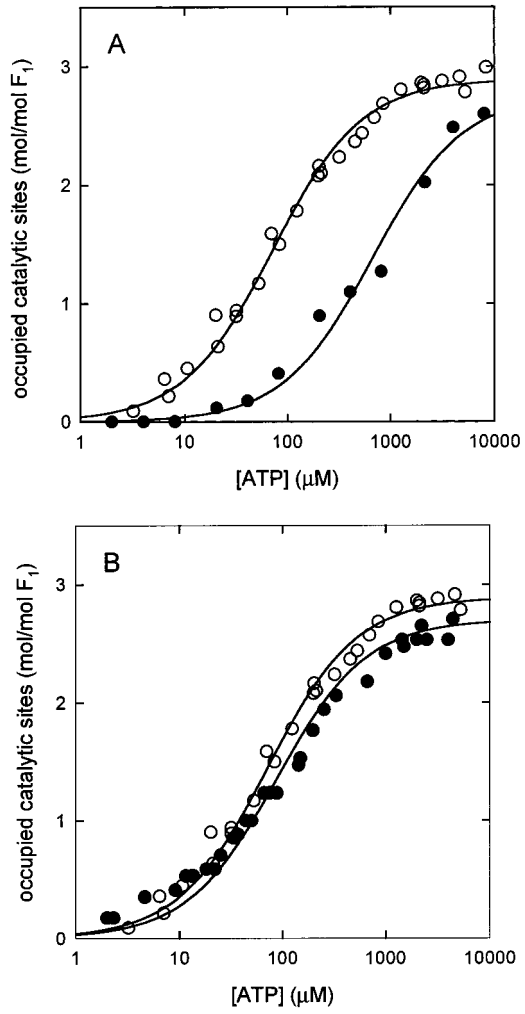

FIGURE 3: ATP binding to catalytic sites of βR182Q/βY331W and βR182K/βY331W F_1: (A) ●, R182Q/βY331W F_1; ○, βY331W F_1; and (B) ●, βR182K/βY331W F_1; ○, βY331W F_1. The lines are computer-generated fits assuming a model with a single type of binding site. Calculated K_d values are given in Table 2. See Experimental Procedures for further details.

fit the data well. Figure 2B and the calculated K_d values (Table 2) indicate that the βR182K mutation had affected MgATP binding only at the highest-affinity site where there was a 5-fold decrease in binding affinity.

ATP Binding to βR182Q/βY331W and βR182K/βY331W F_1. Figure 3A shows the titration curve for free ATP binding to βR182Q/βY331W F_1 (filled circles) compared with

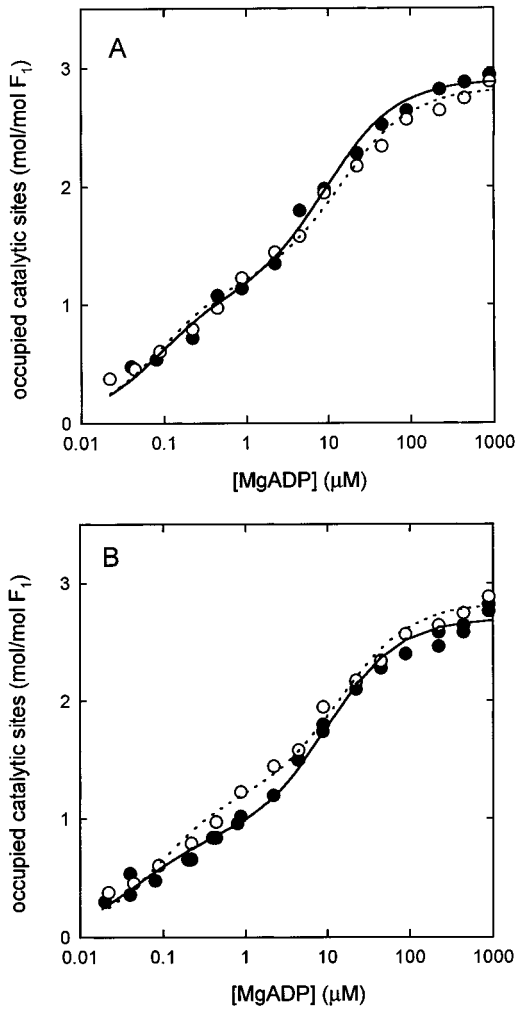

FIGURE 4: MgADP binding to catalytic sites of βR182Q/βY331W and βR182K/βY331W F_1: (A) ●, R182Q/βY331W F_1; ○, βY331W F_1; and (B) ●, βR182K/βY331W F_1; ○, βY331W F_1. The lines (solid for βR182Q/βY331W and βR182K/βY331W F_1; dotted for βY331W F_1) are computer-generated fits assuming a model with two types of binding site. Calculated K_d values are given in Table 2. See Experimental Procedures for further details.

βY331W F_1 (open circles). The lines represent a computer-generated fit for a model with a single class of binding site. One can see that βR182Q/βY331W F_1 had reduced binding affinity for ATP as compared to βY331W F_1. The calculated K_d value (Table 2) reveals that the βR182Q mutation reduced binding affinity for free ATP by about 10-fold. The calculated total number of binding sites, *N*, was 2.8 for βR182Q/βY331W F_1 and 2.9 for βY331W. As can be seen from Figure 3B, there was essentially no difference between the titration curves for free ATP binding to βR182K/βY331W and βY331W F_1. Calculated K_d values are given in Table 2. For βR182K/βY331W F_1 the calculated total number of binding sites was 2.7.

Overall, the MgATP- and ATP-binding data in Figures 2 and 3 indicated that the βR182Q mutation markedly reduced binding affinities for MgATP and free ATP, whereas in contrast the βR182K mutation had no significant effect on free ATP binding and only a minor effect on MgATP binding at catalytic site 1.

MgADP Binding to βR182Q/βY331W and βR182K/βY331W F_1. Figure 4, parts A and B, show MgADP-binding data to βR182Q/βY331W and βR182K/βY331W F_1, respec-

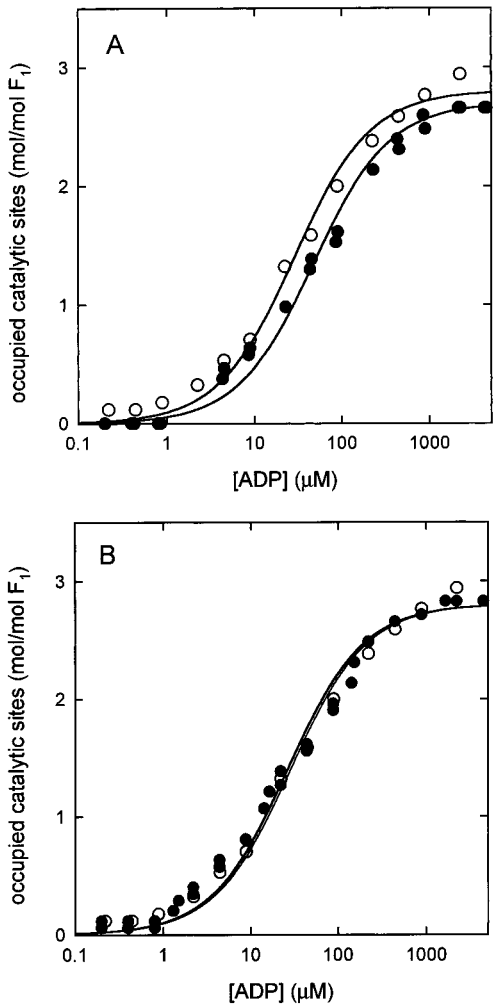

FIGURE 5: ADP binding to catalytic sites of βR182Q/βY331W and βR182K/βY331W F_1: (A) ●, R182Q/βY331W F_1; ○, βY331W F_1; and (B) ●, βR182K/βY331W F_1; ○, βY331W F_1. The lines are computer-generated fits assuming a model with a single type of binding site. Calculated K_d values are given in Table 2. See Experimental Procedures for further details.

tively, and it is clear that neither βR182Q nor βR182K impaired MgADP binding at any of the catalytic sites. The lines (solid for βR182Q/βY331W and βR182K/βY331W; dotted for βY331W F_1) are fits to a model assuming 2 classes of binding sites, a model that has proved satisfactory to describe MgADP binding in previous work (*11*, *16*) and was also satisfactory here. Calculated K_d values are given in Table 2. (The N values for the two classes of sites occupied by MgADP in βR182Q/βY331W F_1 were N_1 (high-affinity site) = 1.1 and N_2 (low-affinity sites) = 1.8; the respective N values for βR182K/βY331W F_1 were 0.9 and 1.8).

ADP Binding to βR182Q/βY331W and βR182K/βY331W F_1. Titration curves for free ADP binding to βR182Q/βY331W and βR182K/βY331W F_1 are shown in Figure 5, parts A and B, respectively. In both cases, the lines are fits to a model assuming a single class of binding site. Calculated K_d values are given in Table 2. The total number of binding sites, N, occupied by ADP was 2.7 for βR182Q/βY331W and 2.8 for βR182K/βY331W F_1. It is evident that neither βR182Q nor βR182K affected free ADP binding significantly at any of the catalytic sites.

To summarize, the binding data for MgADP and free ADP demonstrate that β-Arg-182 is not involved in binding MgADP or ADP at any of the three catalytic sites.

MgADP−Fluoroaluminate Binding to βR182Q/βY331W and βR182K/βY331W F_1. MgADP−fluoroaluminate inhibits F_1-ATPase potently and was suggested to be an analogue of the nucleotide species occurring during the catalytic transition state of the ATP hydrolysis and synthesis reactions in F_1 (*28*−*30*). In a recent study (*16*), we measured MgADP-binding properties of βY331W F_1 in the presence of $AlCl_3$ and NaF to assess possible formation of a transition-state-like intermediate. We found that fluoroaluminate greatly enhanced MgADP-binding affinity at the highest-affinity site (K_{d1} changed from 0.08 μM to $\ll$1 nM). There was also a significant although smaller increase in MgADP-binding affinity at site 2 but no change in affinity at site 3. Two mutant enzymes (βK155Q and βE181Q), in which ATPase activity is essentially inactivated, showed no changes of MgADP binding on addition of fluoroaluminate. From this work we proposed that MgADP−fluoroaluminate binds and mimics the catalytic transition state at site 1, adopts a partial transition-state-like structure at site 2, and does not bind at site 3. Since β-Arg-182 lies in the catalytic site close to the nucleotide phosphates (Figure 1), it is potentially a residue responsible for the stabilization of the catalytic transition state. Hence, MgADP-binding properties of βR182Q/βY331W and βR182K/βY331W F_1 were determined in the presence of $AlCl_3$ and NaF.

Figure 6A shows titration curves for MgADP binding to βR182Q/βY331W F_1 in the presence or absence of $AlCl_3$ plus NaF. It can be seen that the two curves are essentially identical, indicating that fluoroaluminate did not alter the MgADP-binding affinity of βR182Q/βY331W F_1 at any of the three catalytic sites. This is in contrast to the large increase in MgADP-binding affinity shown by βY331W F_1 in the presence of fluoroaluminate (ref *16*, and above). Therefore we conclude βR182Q/βY331W F_1 cannot form the catalytic transition state.

Figure 6B shows titration curves for MgADP binding to nucleotide-depleted βR182K/βY331W F_1 in the presence or absence of $AlCl_3$ plus NaF.[2] It can be seen that in the presence of fluoroaluminate there was a very large increase in binding affinity for MgADP. A model assuming three different classes of binding sites fit well to the data for MgADP binding in the presence of fluoroaluminate (as was seen prevously in ref *16* for MgADP−fluoroaluminate binding to βY331W enzyme), and calculated dissociation constants were the following: $K_{d1} \ll 1$ nM, $K_{d2} = 0.04$ μM, and $K_{d3} = 12.8$ μM. In absence of fluoroaluminate, using the same model, calculated dissociation constants were $K_{d1} = 0.02$ μM, $K_{d2} = 2.0$ μM, and $K_{d3} = 26.7$ μM. (A model assuming two types of binding sites fit these latter data equally well, and the calculated values were $K_{d1} = 0.04$ μM, $N_1 = 1.2$, $K_{d2} = 11.0$ μM, and $N_2 = 1.7$). Thus it is clear that in βR182K/βY331W F_1, fluoroaluminate did affect binding affinity of MgADP. The affinity increased greatly at site 1, significantly at site 2, but not at site 3, similar to what was seen previously in βY331W F_1. Hence, βR182K/βY331W F_1, like βY331W F_1, can form a catalytic transition-state structure.

[2] In cases where fluoroaluminate increases MgADP-binding affinity at catalytic sites, net transfer of nucleotide from noncatalytic to catalytic sites may occur (*16*). Hence completely nucleotide-depleted F_1 (made as in ref *24*) is used in such cases.

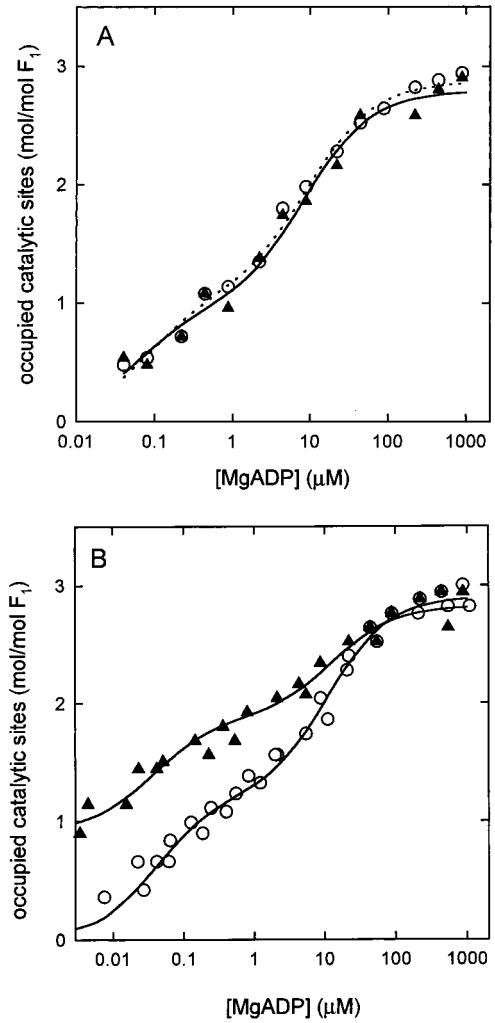

FIGURE 6: MgADP binding to catalytic sites of βR182Q/βY331W and βR182K/βY331W F_1 in the presence or absence of fluoroaluminate: ▲, presence of fluoroaluminate; ○, absence of fluoroaluminate. (A) βR182Q/βY331W: the lines are computer-generated fits assuming a model with two types of binding site. (B) Nucleotide-depleted βR182K/βY331W F_1: the lines are computer-generated fits assuming a model with three types of binding site (▲) or two types of binding site (○).

Summarizing, the data with MgADP−fluoroaluminate show that (a) βR182Q/βY331W F_1 cannot form the catalytic transition state, indicating that β-Arg-182 is one of the residues involved in stabilizing the transition state, yet (b) βR182K/βY331W F_1 can form the transition state, demonstrating that replacement of Arg with Lys still allows formation of the transition state.

DISCUSSION

The aim of this work was to investigate the role of β-Arg-182, a residue essential for catalysis in ATP synthase. The crystal structure of F_1 (*3*) reveals that one of the nitrogens of the guanidinium group of β-Arg-182 lies 3.3 Å from the nearest γ-phosphate oxygen, 6.9 Å from the nearest β-phosphate oxygen, and 3.9 Å from magnesium in the MgAMP-PNP-containing catalytic site. Stacked against the adenine ring of the bound nucleotide is β-Tyr-331 which, when replaced by Trp, acts as an intrinsic fluorescent probe sensitive to nucleotide binding. In this study, we constructed two double mutants, βR182Q/βY331W and βR182K/βY331W, to study the functions of β-Arg-182. In purified F_1 the fluorescence signal of β-Trp-331 is quenched completely when the catalytic site binds nucleotide, making it possible to determine the catalytic site nucleotide equilibrium binding parameters of the double mutant enzymes.

The extremely low rates of steady-state ATPase exhibited by βR182Q/βY331W and βR182K/βY331W F_1 (Table 1) and the absence of oxidative phosphorylation in the mutant strains leave no doubt that β-Arg-182 is crucial for catalysis. There seems to be a strict requirement for Arg at β-182, as even the conservative Lys substitution impaired steady-state ATPase in F_1 by 99%. The low rates of steady-state catalysis reported here are of similar magnitude to those observed in βR182Q and βR182K F_1 by Park et al. (*17*).

Our results demonstrate that β-Arg-182 accelerates catalysis in two major ways: one by providing binding energy for MgATP and the second by stabilizing the catalytic transition state. The first function is indicated by the decrease in MgATP-binding affinity seen when Arg is replaced by the neutral residue glutamine. From the binding affinities in Table 2, calculated MgATP-binding energies contributed by β-Arg-182 are 2.0 kcal/mol at site 1, 1.1 kcal/mol at site 2, and 0.6 kcal/mol at site 3. Interaction of β-Arg-182 with the γ-phosphate of MgATP is strongest at the high-affinity site, where catalysis is thought to occur (*2*). That interaction is primarily with the γ-phosphate is evident from the lack of effect of the mutations on MgADP- or ADP-binding affinity.

The second important role of β-Arg-182 is the stabilization of the transition state. X-ray crystallographic studies showed that MgADP−fluoroaluminate and MgGDP−fluoroaluminate are tight-binding transition-state analogues in myosin (*31*), nucleoside diphosphate kinase (*32*), nitrogenase (*33*), and G proteins (*34*−*38*). Earlier reports (*28*−*30*, *41*) indicated that MgADP−fluoroaluminate binds with a stoichiometry of 2 mol/mol F_1 and suggested that MgADP−fluoroaluminate could be a transition-state analogue in F_1-ATPase. Recent work from our laboratory (*16*) gave strong support to this notion. We have proposed (*16*) that the dramatically increased binding of MgADP−fluoroaluminate at site 1 ($K_{d1} \ll 1$nM) represents binding of a transition state and the increased binding affinity at site 2 could be indicative of a partial transition-state-like structure. Data obtained here with βR182Q/βY331W F_1 (Figure 6A) showed that MgADP-binding affinity was not affected by fluoroaluminate; thus the βR182Q enzyme cannot form the transition state. Clearly, β-Arg-182 is one of the residues necessary for stabilizing the transition state.

β-Arg-182 does not interact with product MgADP, as evidenced from the unaltered MgADP-binding properties of βR182Q/βY331W F_1 (Figure 4A). Neither is it involved in coordinating Mg^{2+} at the catalytic sites, since both MgATP (Figure 2A) and MgADP (Figure 4A) bound in a cooperative, asymmetric manner to βR182Q/βY331W F_1, contrasting with the symmetric binding pattern shown by F_1 mutants which lack functional side chains of residues involved in liganding Mg^{2+}. For example, β-Thr-156, β-Asp-242, and β-Glu-185 have been found to directly or indirectly (via water molecules) coordinate Mg^{2+} at the catalytic sites, and removal of the side chains of any of these residues results in noncooperative (symmetric) binding of both MgATP and MgADP (*14*).

Interestingly, the characteristics displayed by β-Arg-182 in binding MgATP and stabilizing the transition state

resemble those of another positively charged residue in the catalytic site, β-Lys-155. This conserved Lys, which lies in the Walker A motif (P-loop) of the catalytic site (Figure 1), is crucial for catalysis (*39*, *40*), and interacts specifically with the γ-phosphate of MgATP, primarily at catalytic sites 1 and 2 (*15*). Like β-Arg-182, β-Lys-155 also stabilizes the transition state (*16*) and has no significant role in binding MgADP (*15*). Thus, during MgATP hydrolysis, β-Arg-182 and β-Lys-155 provide binding energy for MgATP by interacting with the negatively charged oxygens of the γ-phosphate. As the reaction develops, they stabilize the transition state, but then they have no interaction with the product MgADP. Presumably, during ATP synthesis, changes in catalytic site conformations ("binding changes") cause these two residues to weaken their interaction with the γ-phosphate of MgATP as the site containing MgATP enters the lowest-affinity state, thus enabling newly formed MgATP to be released.

In contrast to βR182Q/βY331W F_1, nucleotide-binding parameters of βR182K/βY331W F_1 were in general similar to those of βY331W F_1. The only impairment of nucleotide binding seen in βR182K/βY331W F_1 was a 5-fold decrease in MgATP-binding affinity at the highest-affinity site. A similar reduction in MgATP-binding affinity (*7*−fold) in βR182K F_1 was reported by Park et al. (*17*). It is unlikely that this small increase in K_{d1} for MgATP could be responsible for the large loss of activity. Furthermore, the βR182K/βY331W enzyme bound MgADP−fluoroaluminate (Figure 6B) in a manner similar to that of βY331W F_1 (*16*). Both enzymes showed dramatic enhancement of MgADP binding by fluoroaluminate at site 1,[3] significant though smaller increase in affinity at site 2, and no change at site 3. Therefore the βR182K/βY331W F_1 appears well able to achieve the catalytic transition state. This is consistent with unisite experiments (*17*) on βR182K F_1, which showed that this enzyme has normal unisite catalysis, with rate constants for hydrolysis and resynthesis of bound MgATP similar to those for wild-type. It is therefore both surprising and intriguing that, despite having near-normal nucleotide-binding parameters and the ability to achieve the transition state, βR182K/βY331W F_1 cannot carry out normal rates of steady-state catalysis.

The location of β-Arg-182 in the catalytic site may provide an answer to this paradox. β-Arg-182 lies at the catalytic site $\beta-\alpha$ interface and is close to several amino acid residues in the adjacent α-subunit (see Figure 1). Specifically, the main-chain carbonyl oxygens of residues α-Ile-346, α-Ser-347, α-Ile-348, and α-Thr-349 all lie within 3.5 Å of the β-Arg-182 guanidinium group in the "βTP" catalytic site (*3*). Hydrogen bonds are likely between β-Arg-182 NH2 nitrogen and the main-chain carbonyl oxygen of α-Thr-349 (distance equals 2.72 Å) and the β-Arg-182 NE nitrogen and the main-chain carbonyl oxygen of residue α-Ile-348 (distance equals 2.96 Å). We have previously demonstrated, from studies on mutations in α-subunit at the catalytic site $\beta-\alpha$ interface, that conformational changes transmitted across this interface are essential for and integral to steady-state, multisite catalysis (reviewed in ref *2*). Supporting the idea that movement of residues occurs at this interface, Abrahams et al. (*3*) found that another residue in this region, α-Arg-376, which lies very close to the nucleotide phosphates, takes up a different position depending upon whether nucleoside di- or tri-phosphate occupies the catalytic site. Interaction of β-Arg-182 with α-Ile-348 and/or α-Thr-349 could be important for maintaining this function. Thus, substitution of β-Arg-182 by Lys could still provide positive charge to support close to normal binding of nucleotide and stabilization of the transition state, but lacking the guanidinium group, it may not be able to form important interactions with α-Thr-349 or other residues across the $\beta-\alpha$ interface. Hence, while neither its ability to bind nucleotide nor its ability to stabilize the transition state is impaired, βR182K/βY331W F_1 fails to reach wild-type rates of steady-state catalysis.

[3] We do not have exact estimates of K_{d1} in either βR182K/βY331W or βY331W enzyme because the Mg−fluoroaluminate-binding affinity at site 1 is very high, so they may differ.

ACKNOWLEDGMENT

This work was supported by NIH Grant GM25349 to A.E.S. We thank Rachel Shaner for excellent technical assistance.

REFERENCES

1. Nakamoto, R. K. (1996) *J. Membr. Biol. 151*, 101−111.
2. Weber, J., and Senior, A. E. (1997) *Biochim. Biophys. Acta 1319*, 19−58.
3. Abrahams, J. P., Leslie, A. G. W., Lutter, R., and Walker, J. E. (1994) *Nature 370*, 621−628.
4. Noji, H., Yasuda, R., Yoshida, M., and Kinosita, K., Jr. (1997) *Nature 386*, 299−302.
5. Yasuda, R., Noji, H., Kinosita, K., Jr., Motojima, F., and Yoshida, M (1997) *J. Bioenerg. Biomembr. 29*, 207−209.
6. Weber, J., Wilke-Mounts, S., and Senior, A. E. (1994) *J. Biol. Chem. 269*, 20462−20467.
7. Boyer, P. D. (1989) *FASEB J. 3*, 2164−2178.
8. Penefsky, H. S., and Cross, R. L. (1991) *Adv. Enzymol. 64*, 173−214.
9. Bianchet, M. A., Hullihen, J., Pedersen, P. L., and Amzel, L. M. (1998) *Proc. Natl. Acad. Sci. U.S.A. 95*, 11065−11070.
10. Shirakihara Y., Leslie, A. G. W., Abrahams, J. P., Walker, J. E., Ueda, T., Sekimoto, Y., Kamabara, M., Saika, K., Kagawa, Y., and Yoshida, M (1997) *Structure 5*, 825−836.
11. Weber, J., Wilke-Mounts, S., Lee, R. S. F., Grell, E., and Senior, A. E. (1993) *J. Biol. Chem. 268*, 20126−20133.
12. Weber, J., Bowman, C., and Senior, A. E. (1996) *J. Biol. Chem. 271*, 18711−18718.
13. Weber, J., Wilke-Mounts, S., Hammond, S. T., and Senior, A. E. (1998) *Biochemistry 37*, 12042−12050.
14. Weber, J., Hammond, S. T., Wilke-Mounts, S., and Senior, A. E. (1998) *Biochemistry 37*, 608−614.
15. Löbau, S., Weber, J., Wilke-Mounts, S., and Senior, A. E. (1997) *J. Biol. Chem. 272*, 3648−3656.
16. Nadanaciva, S., Weber, J., and Senior, A. E. (1999) *J. Biol. Chem. 274*, 7052−7058.
17. Park, M. Y., Omote, H., Maeda, M., and Futai, M. (1994) *J. Biochem. 116*, 1139−1145.
18. Vandeyar, M., Weiner, M., Hutton, C., and Batt, C (1988) *Gene 65*, 129−133.
19. Lee, R. S. F., Pagan, J., Wilke-Mounts, S., and Senior A. E. (1991) *Biochemistry 30*, 6842−6847.
20. Ketchum, C. J., Al-Shawi, M. K., and Nakamoto, R. K. (1998) *Biochem. J. 330*, 707−712.
21. Senior, A. E., Latchney, L. R., Ferguson, A. M., and Wise, J. G. (1984) *Arch. Biochem. Biophys. 228*, 49−53.
22. Rao, R., Al-Shawi, M. K., and Senior, A. E. (1988) *J. Biol. Chem. 263*, 5569−5573.
23. Weber, J., Lee, R. S. F., Grell, E., Wise, J. G., and Senior, A. E. (1992) *J. Biol. Chem. 267*, 1712−1718.
24. Senior, A. E., Lee, R. S. F., Al-Shawi, M. K., and Weber, J. (1992) *Arch. Biochem. Biophys. 297*, 340−344.
25. Laemmli, U. K. (1970) *Nature 227*, 680−685.
26. Bradford, M. M. (1976) *Anal. Biochem 72*, 248−254.

27. van Veldhoven, P. P., and Mannaerts, G. P. (1987) *Anal. Biochem. 161*, 45−48.
28. Lunardi, J., Dupuis, A., Garin, J., Issartel, J. P., Michel, L., Chabre, M., and Vignais, P. V. (1988) *Proc. Natl. Acad. Sci. U.S.A. 85*, 8958−8962.
29. Dupuis, A., Issartel, J. P., and Vignais, P. V. (1989) *FEBS Lett. 255*, 47−52.
30. Issartel, J. P., Dupuis, A., Lunardi, J., and Vignais, P. V. (1991) *Biochemistry 30*, 4726−4733.
31. Fisher, A. J., Smith, C. A., Thoden, J. B., Smith, R., Sutoh, K., Holden, H. M., and Rayment, I. (1995) *Biochemistry 34*, 8960−8972.
32. Xu, Y. W., Morera, S., Janin, J., and Cherfils, J. (1997) *Proc. Natl. Acad. Sci. U.S.A. 94*, 3579−3583.
33. Schindelin, H., Kisker, C., Schlessman, J. L., Howard, J. B., and Rees, D. C. (1997) *Nature 387*, 370−376.
34. Rittinger, K., Walker, P. A., Eccleston, J. F., Smerdon, S. J., and Gamblin, S. J. (1997) *Nature 389*, 758−762.
35. Scheffzek, K., Ahmadian, M. R., Kabsch, W., Wiesmüller, L., Lautwein, A., Schmitz, F., and Wittinghofer, A. (1997) *Science 277*, 333−338.
36. Sondek, J., Lambright, D. G., Noel, J. P., Hamm, H. E., and Sigler, P. B. (1994) *Nature 372*, 276−279.
37. Coleman, D. E., Berghuis, A. M., Lee, E., Linder, M. E., Gilman, A. G., and Sprang, S. R. (1994) *Science 265*, 1405−1412.
38. Tesmer, J. J. G., Berman, D. M., Gilman, A. G., and Sprang, S. R. (1997) *Cell 89*, 251−261.
39. Senior, A. E., and Al-Shawi, M. K. (1992) *J. Biol. Chem. 267*, 21471−21478.
40. Senior, A. E., Wilke-Mounts, S., and Al-Shawi, M. K. (1993) *J. Biol. Chem. 268*, 6989−6994.
41. Dou, C., Grodsky, N. B., Matsui, T., Yoshida, Y., and Allison, W. S. (1997) *Biochemistry 36*, 3719−3727.

BI990663X